DOI: 10.13009/EUCASS2019-428

Post-Flight Evaluation of the Guidance and Control for Re-entry Capsule "HSRC"

Misuzu HARUKI, Ryo NAKAMURA* and Shuichi MATSUMOTO**
*Satoshi KOBAYASHI** and Issei KAWASHIMA**, Kotaro AOKI*** and Nobuaki KIKUCHI ****
** Japan Aerospace Exploration Agency 2-1-1 Sengen, Tsukuba-shi, Ibaraki 305-8505*
haruki.misuzu@jaxa.jp, nakamura.ryoh@jaxa.jp, matsumoto.shuichi@jaxa.jp
*** Mitsubishi Space Software Co., Ltd. Tsukuba Mitsui Bldg.,1-6-1, Takezono, Tsukuba-shi, Ibaraki-ken 305-0032*
Kobayashi.Satoshi@mss.co.jp, Kawashima.Issei@mss.co.jp
**** Mitsubishi Heavy Industries, Ltd. 10-5, Oye-cho, Minato-ku, Nagoya, 455-8515, Japan*
kotaro_aoki@mhi.co.jp, nobuaki_kikuchi@mhi.co.jp

Abstract

In this paper, we give the GN&C system design of Small Re-entry Capsule (HSRC) integrated into HTV and describe the post-flight evaluation results. HSRC including samples was successfully recovered from the ISS in November 2018. One key design of GN&C system is its re-entry guidance logic for range control using bank angle modulation with a low L/D. The guidance logic determinate commanded bank based on range predicted in real-time using numerical integration. The flight results confirmed that the proposed guidance logic effectively reduces the maximum aerodynamic acceleration during flight and improves guidance accuracy.

1. Introduction

1.1 Objective of HSRC project

Small Re-entry Capsule integrated into HTV (HSRC) is Japan's first re-entry capsule developed to return samples from the International Space Station (ISS) [1]. On November 11, 2018, Japan Aerospace Exploration Agency (JAXA) succeeded in its HSRC flight demonstration. HSRC is about 0.8 m in diameter, making it the world's smallest re-entry vehicle from low Earth orbit (LEO). Figure 1 illustrates the HSRC mission sequence from launch to recovery. HSRC re-entry trajectory was direct re-entry not Skip trajectory. HTV conducts an orbital transition from LEO to re-entry orbit and has successfully completed the past six re-entries with high re-entry accuracy at the re-entry interface. The HSRC is responsible for its control and guidance after separation from the HTV.

The guidance and control team had two requirements for returning samples. One is the reduction of maximum aerodynamic acceleration during flight. For the same size, weight, and re-entry conditions as those of HSRC in ballistic flight, maximum aerodynamic acceleration of about 8 G or more is assumed for the capsule. To maintain the quality of the samples, maximum aerodynamic acceleration during flight must be reduced to 4G or less. The other requirement is pinpoint landing. The re-entry capsule must return near the target point so that the recovery ship can stably and smoothly recover it. Therefore, the team was required improved guidance accuracy to a given target point.

Previous Japanese capsules included OREX (Orbital Re-entry EXperiment) [2], USERS capsule [3], and HAYABUSA re-entry capsule [4]. However, ballistic re-entry capsules have resulted in a large splashdown area and high maximum aerodynamic acceleration. Consequently, the guidance and control team faced the challenge of designing a guidance, navigation and control (GN&C) system for a small re-entry capsule, including guidance logic that uses real-time predictive integration for range control. Thus, we applied the guidance logic to reduce maximum aerodynamic acceleration and improve guidance accuracy.

DOI: 10.13009/EUCASS2019-428

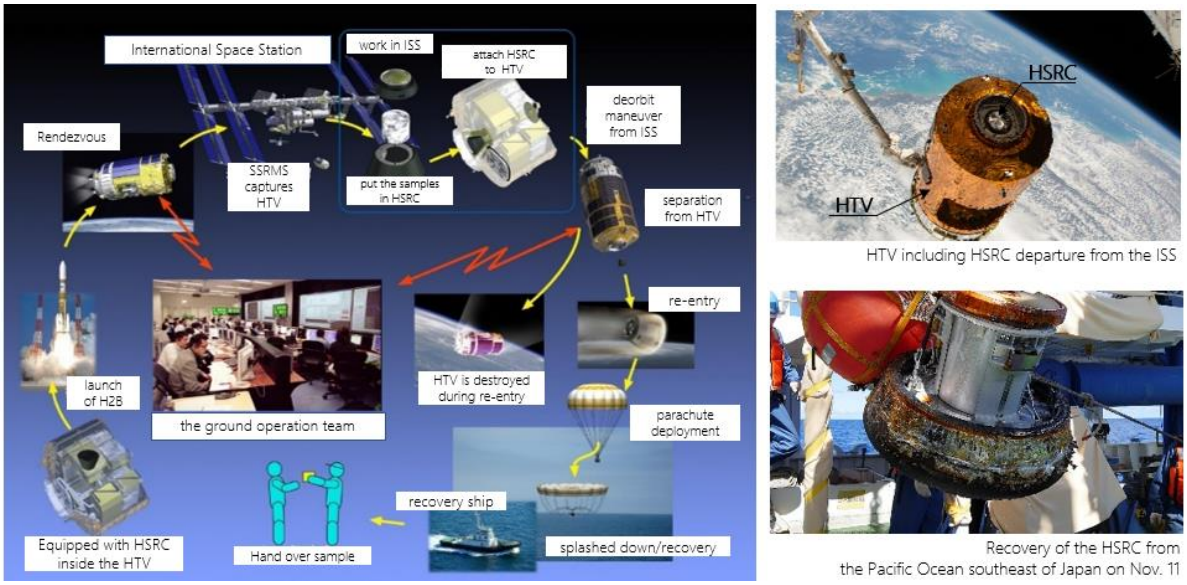

Figure 1: HSRC mission sequence from launch to recovery

1.2 Guidance logic for low L/D re-entry capsule

Guidance logic during re-entry from an altitude 120km or less for low L/D capsule has been demonstrated in Apollo [5,6], Orion capsule [7,8], MSL [9,10] etc. The logic of these capsules was the guidance logic based on Apollo's final phase. The guidance uses a reference trajectory. Bank command is determined using deviation from the reference trajectory and control gains [5]. The guidance logic is very effective. The guidance has been thoroughly flight-tested and the calculation load is low. Since the reference trajectory is generated based on the reference L/D, when applying this logic, it is important that the L/D with sufficiently high accuracy be known.

The guidance logic demonstrated on HSRC is the real-time prediction guidance using numerical integration. This guidance logic has been studied by Matsumoto et al [11]. It offers the advantages of high accuracy and robustness against errors. The guidance logic does not use a reference trajectory, but instead generates trajectories from the current state including the commanded bank in each cycle. The guidance method can perform bank angle modulation to reduce the down-range error even in case of high uncertainty, such as aerodynamic modeling errors. Our previous research compared the variable gain guidance logic and the real-time induction logic [11]. As a result, both robustness and accuracy were found to be good against highly uncertain aerodynamic errors.

One GNC design challenge was that the L/D error was assumed to be large due to the capsule's small size. The shape change due to recession is assumed to be large compared to the original size, resulting in L/D error during flight. And to generate the necessary L/D, adjusting the center of gravity position (balance adjustment or measurement) is important. Given the small size of the HSRC, its sensitivity to L/D is high and difficult. Therefore, the GN&C system of HSRC must be designed by considering errors caused by its design and manufacture (i.e., large L/D error).

From the above, we emphasize the robustness against highly uncertain errors and adopted the guidance logic using the real-time predictive integration for range control. This paper gives the design of the GN&C system including the guidance logic and describes the post-flight evaluation results of the guidance and control. Actual flight results confirmed that the proposal guidance logic effectively reduced maximum aerodynamic acceleration during flight and improves guidance accuracy.

1.3 Relevant terminology and the scope of this paper

In this paper, the meanings of the terms "down-range" and "cross-range" are as follows: The term "down-range" means that the capsule flight distance in flight plane in local horizontal plane. The term "cross-range" means that the capsule flight distance out flight plane in local horizontal plane.

DOI: 10.13009/EUCASS2019-428

The remainder of the present paper is organized as follows. Chapter 2 introduces the vehicle model of the HSRC. Chapter 3 states Mission requirement of GN&C system. Chapter 4 reviews design of GN&C system including trajectory design. Chapter 5 describes the real-time prediction guidance using numerical integration for re-entry. In the chapter 6, we present and discuss the flight results of HSRC. In the chapter 7, reconstruction trajectory is presented. This paper summary is described in Chapter 8.

2. Vehicle model

We introduce the vehicle model and the aerodynamic characteristics of HSRC in this chapter. Both models are an important prerequisite to design the GNC system. HSRC is axisymmetric shape with an offset centre of gravity location such as Apollo or Orion capsule. The vehicle flies at an attack angle and generates lift as well as drag. HSRC is designed to generate a lift-to-drag ratio(L/D) of 0.2-0.3 during re-entry flight. The left figure in Figure 2 shows the shape of HSRC. The mass is 197.8 kg, the reference length (capsule diameter) is 0.84 m and the reference cross section is 0.5542 m^2.

The right figure in Figure 2 shows the aerodynamic characteristics (trim angle) of HSRC in flight. The aerodynamic characteristics of HSRC have two features. One is the large impact of recession. Recession is a phenomenon that changes the shape due to ablation at re-entry. Recession result in pitching down moment, so that the effect of the re-entry capsule's recession increases the absolute value of the trim angle and the trim L/D. For large capsules, there is a small amount of change in shape due to recession compared to the original size. Because HSRC is small, however, there is a large amount of change in shape, which affects its L/D.

The other feature is rolling moment coefficient. As HSRC is axisymmetric shape, the nominal rolling moment coefficient is 0.0. However, the rolling moment was confirmed in wind tunnel test results of 3 degrees of freedom. And in the Orion Crew Module Static Aerodynamic database, rolling moment uncertainty was considered based on historical considerations [12]. Consequently, HSRC aerodynamic database consider rolling moment coefficient.

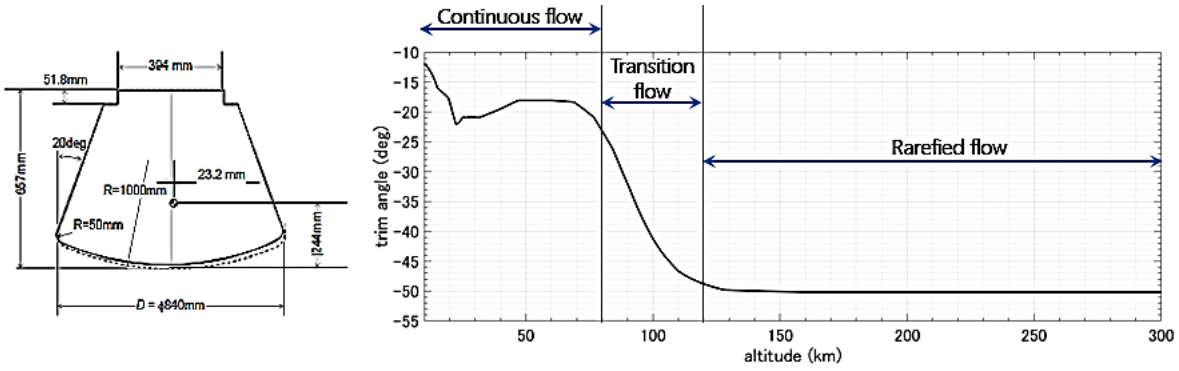

Figure 2: Vehicle model (the shape and trim angle of HSRC)

3. Mission requirement of GN&C system

The main mission of HSRC is to return samples from ISS to Earth. To achieve the mission, the GNC system must satisfy all of the requirements listed below. Note that "(done by OREX)" means that the requirement has already been demonstrated in OREX. Also note that "(HSRC)" marks the first challenge in Japan.

- Navigation calculation of position and attitude by IMU（done by OREX）
- Three-axis attitude control using Reaction Control System (RCS) thrusters during re-entry flight (HSRC)
- Trajectory design for stable capsule flight with low L/D (HSRC)
- Demonstration the guidance logic, which is range control using real-time prediction guidance based on numerical integration (HSRC)
  - Reduction of maximum aerodynamic acceleration using the guidance logic (less 4G)
  - Improvement of guidance accuracy using the guidance logic (within 10 km at guidance termination)
  - Improvement of guidance accuracy using the guidance logic (within 10km at termination guidance)
- Flight sequence design from LEO to parachute deployment, especially the output trigger to meet parachute

DOI: 10.13009/EUCASS2019-428

deployment conditions (HSRC)

4. Design of GN&C system

4.1 Configuration

The GN&C system of HSRC consists of one Inertial Measurement Unit (IMU), one Global Positioning System (GPS) receiver, one GPS antenna, and one flight computer with GNC flight software installed. The GNC flight software consists of four modules—system module, control module, navigation module and guidance module. The system module has the output event trigger and FDIR (Fault Detection, Isolation and Recovery) functions. The torques for three-axis attitude control are generated by eight cold gas thrusters, four rolls, two pitches and two yaws. Eight thrusters that generate 2.4N of thrust each are mounted on the capsule side wall.

4.2 Trajectory design

Flight sequence
Figure 3 illustrates the flight sequence of events. The re-entry flight of HSRC is direct entry into Earth's atmosphere from LEO. HSRC was transferred by HTV from ISS into re-entry orbit, and then separated from HTV at an altitude of about 300km. The flight sequence is divided into two phases: on-orbit-phase and re-entry-phase.
In each phase, the flight sequence of HSRC is designed to perform the following actions:

In on-orbit-phase,
- Start navigation 10 seconds before separation from HTV
- Change its attitude to direct the GPS antenna to the zenith direction and perform initial acquisition of GPSR
- Maneuver into the re-entry attitude

In re-entry-phase,
- Start the control range using real-time prediction guidance based on numerical integration
- Terminate guidance at the flight target altitude of approximately 30km.
- Perform rate dumping for 100 seconds after stopping guidance calculation
- Output the trigger of parachute deployment at an altitude of about 11km (near M0.7)

After parachute deployment, HSRC notifies the ground operation team of its location via iridium communication. HSRC is then recovered by ship, after splashdown into the Pacific Ocean.

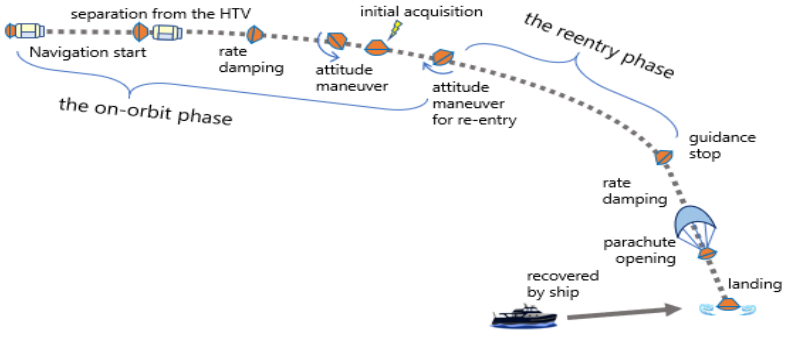

Figure 3: HSRC flight sequence of events

Targeting
Targeting of HSRC in on-orbit-phase is to perform calculation “the target-point” (i.e., defined latitude, longitude, and altitude at guidance termination). We cannot update target location information for HSRC before its re-entry, despite that the HTV de-orbit trajectory cannot be determined until a few days before re-entry. This is because there is no communication method with HSRC after it has been loaded into HTV about six months prior to the launch. Therefore, our trajectory design has two big characteristics. First, we try to fix the shape of re-entry trajectory (i.e., height, ground speed, flight path angle, and azimuth angle) by properly designing the HTV de-orbit maneuvers. Second, HSRC is designed to fly towards the target point which is calculated on orbit using its own navigation and the preset “target-flight-distance” (i.e., down-range when HSRC flies at the nominal bank angle). Because of these methods, even if

DOI: 10.13009/EUCASS2019-428

the absolute position at the separation from HTV is slightly shifted, HSRC can fly toward the target point. In the bank angle range of 0 to 90 degrees, the bank angle at which the down range distance is averaged is 60 deg. The nominal bank angle is 60deg to achieve the center of HSRC range capability.

Attitude maneuver before re-entry phase
The capsule controls its attitude for re-entry flight at an altitude of about 120km. The commanded attack angle is 18.3deg. The value is the trim angle at the start of the guidance. The command sideslip angle is 0 deg. The commanded bank angle is a constant value with the nominal bank angle (60 deg). The sign of the commanded bank angle is determined using heading angle (see Eq. (3)), which is defined as the deviation of the flight direction vector relative to the target-point.

Trigger to start guidance
The GNC Flight Software starts to calculate the guidance for pinpoint landing when the IMU detects 2.0m/s^2 or more. Guidance starts at an altitude is about 70-80km. The trigger is designed to be output after the trim angle becomes constant as shown in the right figure in Fig. 2, because the trim angle is reduced in the transition flow area. If the guidance starts when the trim angle is decreasing, the predict-range error becomes large.

Trigger to terminate guidance and deploy the parachute
The guidance is terminated when the ground speed navigation value decreases to 900 m/s at an altitude of about 30 km. HSRC drops its altitude to meet the parachute deployment conditions (near Mach 0.7). The control is rate dumping from guidance termination to parachute deployment.

4.3 Guidance Navigation and Control

Guidance longitudinal motion
In this section we explain the guidance command for longitudinal motion. chapter 5 describes the guidance logic for range control in detail. The HSRC has a wide flight range (altitude of 300-10 km, The common logarithm of Knudsen number ($\log_{10}$Ku) 2.0-0.4, Mach 10-0.6). The trim angle changes according to the Mach number or Knudsen number (see the right figure in Figure 2). The commanded attack angle is the trim angle as per nominal ground speed scheduling. The command sideslip angle is 0 deg. We also evaluated the longitudinal stability in pre-analysis and confirmed that HSRC can fly steady within the expected error model range by Monte Carlo Simulation.

Navigation
Navigation of HSRC starts 10 seconds prior to separation from HTV7 and calculates until parachute opening. The main navigation is IMU inertial navigation (IMU-nav). In addition, the flight software has IMU/GPS integrated navigation (IMU/GPS-nav) mode and IMU/Drag-Measurement integrated navigation (IMU/DM-nav) mode. The flight software switches between three navigation modes according to the flight sequence. Each logic refers to the paper [11]. In the paper we explain the reasons why IMU/DM-nav and IMU/GPS-nav are applied.

The IMU-nav of HSRC is based on the navigation logic of such Japanese rockets as the H2 and H2A. The logic has been thoroughly flight tested. The attitude quaternion is updated integrating the angular increment of the gyro at 50 Hz. The position and velocity vector in the inertial coordinate system are calculated at 1Hz using velocity increment and gravitational acceleration.

The flight software switches the navigation mode from IMU-nav to IMU/GPS-nav, while the GPSR is available in the on-orbit phase. IMU/GPS-nav estimates the amount of correction by Kalman filter, and updates the navigation value by IMU-nav. The observation parameters are the clock bias and clock drift of the GPSR, and the pseudo-range and delta-range of each GPS satellite. The reason to adopt IMU/GPS-nav is to improve navigation accuracy and consequently guidance accuracy. In case of large navigation errors, especially in ground speed or flight path angle, the down-range error at guidance termination is large. Therefore, it is necessary that navigation is updated is using the IMU/GPS-nav before re-entry. On the other hand, even if the GPSR is recaptured after a blackout, the flight software does not switch from IMU-nav to IMU/GPS-nav. The reason why is to avoid a rapid change in the command attitude when a large amount of correction is estimated IMU/GPS-nav.

The flight software switches the navigation mode from IMU-nav to IMU-DM-nav at an altitude from 70 km to 45 km. IMU/DM-nav is used for improving altitude navigation accuracy before the parachute opens. IMU/DM-nav estimates altitude using drag acceleration observations detected by the IMU, and updates the navigation value by IMU-nav. This logic uses the density model and axial force coefficient (CA). If those models differ significantly from the actual flight, navigation accuracy is not improved. However, altitude navigation accuracy by IMU/DM-nav is better than that of

DOI: 10.13009/EUCASS2019-428

IMU-nav when considering the error factor assumed in actual HSRC flight according to the pre-analysis. For the above reasons, IMU/DM nav is adopted to improve altitude navigation which is used the event triggers of guidance termination and parachute opening.

Control

The flight software performs attitude control calculation in each axis at 50 Hz. We adopt the switching control law for attitude control, which is a control law that turns on the thruster when the attitude angle error or angler velocity exceeds the range of the switching line. The switching line (i.e., switching function) is designed by two control parameters that determine attitude and angular velocity tracking performance.

The biggest program in control is how to reduce fuel consumption. There is not much the cold gas mounted for attitude control, given the HSRC's small size. There are two main causes of fuel consumption being increased within the range of expected errors. One is navigation error (e.g., initial attitude error, gyro bias). In case of large navigation errors, the difference between the commanded angle and the navigation value become large, resulting in increased fuel consumption. The other main cause is rolling moment coefficient, which causes a steady disturbance torque in the roll direction. The disturbance torque becomes large in line with an increase in density. As a result, fuel consumption is increased as the control keeps blowing the roll thrusters against the disturbance torque. To reduce fuel consumption, we design the control as follows: First, longitudinal motion control in the re-entry phase is not actively controlled by widening the dead-band on both the angle of attack and sideslip. The capsule is longitudinally stable during re-entry flight. Next, the control parameters are designed differently according to the capsule's ground speed. Widening the dead-band at the end of the flight suppresses the increase in fuel consumption. During bank reversal, the flight software switches the control parameters to improved attitude tracking performance.

5. Real-time Prediction Guidance using Numerical Integration for re-entry

In this chapter, we explain the guidance logic for range control. The primary object of the guidance logic in the re-entry phase is to reduce the range-to-target error at the target altitude (30 km). The guidance logic controls the range-to-target using bank angle modulation with a small lift-to-drag ratio (L/D) of about 0.2~0.3. The guidance logic is divided into the down-range guidance and the cross-range guidance as two independent processes. The flight software performs the guidance calculation at 1Hz. The guidance calculation is stopped at an altitude of 30 km or less.

5.1 Down-range guidance using numerical integration

When acceleration of 2.0m/s^2 or more is detected by the IMU, the flight software switches from the on-orbit phase to the re-entry phase, and starts to calculate the commanded bank using real-time predictive integration for a pinpoint landing. The altitude of phase transition is about 70~80km.

The guidance algorithm controls the target-to-range using bank angle modulation. In other words, the guidance calculates "how much L/D in-plane" is needed to fly the target range and determines the commanded bank to realize flight with the L/D in-plane. The term "in-plane" means in flight plane in local horizontal plane. The L/D in-plane equals the cosine of the bank angle. Figure 4 shows a schematic diagram of real-time prediction guidance using numerical integration.

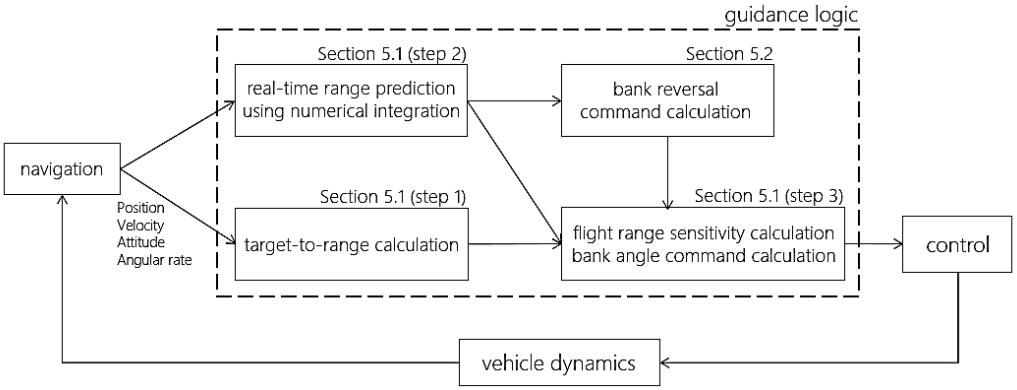

Figure 4: Schematic Diagram of Real-time Prediction Guidance using Numerical Integration

DOI: 10.13009/EUCASS2019-428

There are two points in the guidance logic. One is the method of calculating the bank angle command to meet the required flight range as expressed by Eq. (2). The equation uses "flight range sensitivity around small bank angle". In other words, the guidance calculates the flight range sensitivity when the bank angle is changed by 1 deg. The commanded bank angle needed to reduce the difference between the predicted-range and the range-to-target is calculated. The calculation is performed in each cycle.

The other point is the method of calculating the prediction range-to-go. We adopt numerical integration using the fourth order Runge-Kutta method to improved prediction accuracy. The equations for prediction the trajectory are three degrees of freedom equations of motion as expressed in Eq. (1-1) ~ (1-7). The problem posed by numerical integration is its heavy computing time load. Therefore, we developed logic in which the calculation load is reduced by making integration time variable according to the distance to the target. According to previous study [11], We have an evaluation result that the calculation load is small by this method, and the logic can be applied on the onboard computer.

Details of the algorithm are given below. The algorithm is divided into three steps.
(Step 1) Calculation the target-to-range R_{TGT}
The target-to-range describes the distance between the current position and the target-point. The target-to-range is given as $R_{TGT} = R_{AVE}\,\eta$, where: R_{AVE} is the average value of the geocentric distance between the capsule and the target-point, and η is the angle between the target vector and the navigation vector in inertial coordinate system.

(Step 2) Calculation the predicted range using numerical calculation
In this step, the predicted range is calculated using numerical calculation by the fourth order Runge-Kutta method. The equation of motion of HSRC can be written as shown below. The guidance logic performs the numerical calculation twice to calculate the range sensitivity to $\Delta\phi$ in Step 3: The guidance logic calculates the predicted range $R(\phi_{BC})$ at bank angel ϕ_{BC}, and also calculates the predicted range $R(\phi_{BC}+\Delta\phi)$ at bank angel $(\phi_{BC}+\Delta\phi)$.

$$\frac{dR}{dt} = \mathrm{u} \tag{1-1}$$

$$\frac{dr}{dt} = \mathrm{v} \tag{1-2}$$

$$\frac{d\lambda}{dt} = \frac{\mathrm{u}\sin\psi'}{r\cos\phi_c} \tag{1-3}$$

$$\frac{d\phi_c}{dt} = \frac{\mathrm{u}\cos\psi'}{r} \tag{1-4}$$

$$\frac{dv}{dt} = a_x^H + g_x^H + \frac{u}{r^2} + 2\omega_e u\cos\phi_{BC}\sin\psi' + r{\omega_e}^2(\cos\phi_c)^2 \tag{1-5}$$

$$u\frac{d\psi'}{dt} = a_y^H + g_y^H + \frac{u^2\sin\psi'\tan\phi_c}{r} - 2\omega_e(\mathrm{v}\cos\phi_c\cos\psi' - \mathrm{u}\sin\phi_c) + \mathrm{r}{\omega_e}^2\sin\phi_c\cos\phi_c\sin\psi' \tag{1-6}$$

$$\frac{du}{dt} = a_z^H + g_z^H - \frac{uv}{r} - 2\mathrm{v}\omega_e\cos\phi_c\sin\psi' - \mathrm{r}{\omega_e}^2\sin\phi_c\cos\phi_c\cos\psi' \tag{1-7}$$

R, r : Range, geocentric distance
u, v : Horizontal component and vertical component of ground speed
ϕ_c, λ : Geocentric latitude and longitude
γ', ψ' : Flight path angle and flight azimuth in geocentric horizontal coordinate system
a^H, g^H : Aerodynamic acceleration and Gravity acceleration in the flight plane coordinate system
ω_e : Earth rotation speed

(Step 3) Determining the commanded bank using flight range sensitivity to the bank angle ($\Delta\phi$)
In this step, the guidance logic determines commanded bank ϕ_{BC} to adjust the difference in range ($R_{TGT} - R_{NAV}$).

$$\cos(\phi_{BC1}) = \cos(\phi_{BC}) + \frac{\left(\cos(\phi_{BC}+\Delta\phi) - \cos(\phi_{BC})\right)}{R(\phi_{BC}+\Delta\phi) - R(\phi_{BC})}\left(R(\phi_{BC}) - R_{TGT}\right) \tag{2}$$

ϕ_{BC1} : Bank angle command of next guidance cycle
ϕ_{BC} : Bank angle command of present guidance cycle
$\Delta\phi$: Increment of bank angle for calculation for range sensitivity
R_{TGT} : The target-to-range
$R(\phi_{BC})$: Predicted range from present position when the capsule flies at bank command (ϕ_{BC0})
$R(\phi_{BC}+\Delta\phi)$: Predicted range from present position when the capsule flies at bank command $(\phi_{BC0}+\Delta\phi)$

DOI: 10.13009/EUCASS2019-428

5.2 Cross-range guidance using bank reversal

The cross-range is guided by bank reversals. Bank reversal refers to changing the sign of the bank angle command and adjusting the flight direction. The guidance law evaluates cross-range error by monitoring the heading angle ψ shown in Eq. (3). The guidance law outputs the trigger of bank reversal when the magnitude of the heading angle exceeds the dead-band. Figure 5 shows the bank reversal dead-band as scheduled by the ground speed of HSRC. We design to avoid bank reverse in two ground speed ranges. One is around Mach 1. The airflow around the capsule becomes complicate when it passes through M 1. We consider it undesirable to change the airflow by attitude control. The other is range from 2000 to 3000m/s, where dynamic pressure increases. Such maneuvers as bank reverse change the total attack angle and CL, and increase aerodynamic acceleration. Therefore, we expanded the dead-band threshold from 2000 to 3000m/s to avoid bank reversal.

$$\psi = \sin^{-1}\left\{\frac{\mathbf{r_c}\times\mathbf{r}}{|\mathbf{r_c}\times\mathbf{r}|}\cdot\frac{\mathbf{v_a}}{|\mathbf{v_a}|}\right\} \tag{3}$$

$\mathbf{r_c}$: Vector indicating target-point in inertial coordinate system
$\mathbf{r}$: Position vector in inertial coordinate system
$\mathbf{v_a}$: Ground speed vector in inertial coordinate system

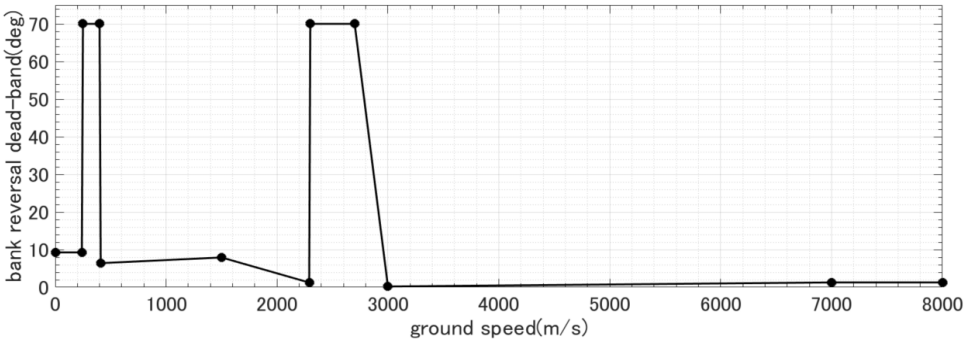

Figure5: The bank reversal dead-band profile

6. Flight results of HSRC

We report the flight result of HSRC in this chapter. The flight results achieved the following in the demonstration.

Achievements

- Demonstrated three-axis attitude control using Reaction Control System (RCS) thrusters during re-entry flight
- Demonstrated the guidance logic, which is range control using real-time prediction guidance based on numerical integration
- Achieved reduced maximum aerodynamic acceleration using the guidance logic
- Achieved improved guidance accuracy using the guidance logic
- Demonstrated stable capsule flight with low L/D
- Demonstrated the flight sequence event from on orbit to parachute opening

However, the flight does not demonstrate initial acquisition of GPSR and navigation by the IMU/GPSR. The project succeeded in recovering the capsule including the samples, thus marking Japan's first successful demonstration of guiding a re-entry capsule. Moreover, the GN&C system including the proposal guidance logic worked well for the small re-entry capsule. And actual flight results shown in Section 6 confirmed that the guidance logic effectively reduced the maximum aerodynamic acceleration during flight and improved the guidance accuracy.

6.1 Flight trajectory

Figure 6 shows the mission trajectory of HSRC and the times of events during the HSRC's flight. On November 11, 2018, HTV7 separated HSRC as planned. HSRC deployed its parachute 1513 seconds after separation and splashed down into the Pacific Ocean near Minamitori-shima. HSRC transmitted the positional information to the ground

DOI: 10.13009/EUCASS2019-428

operation team until recovery ship arrived. We visually confirmed that HSRC returned to Earth at 10:25(JST) and was recovered. The place where HSRC splashed down was in the pre-set landing area.

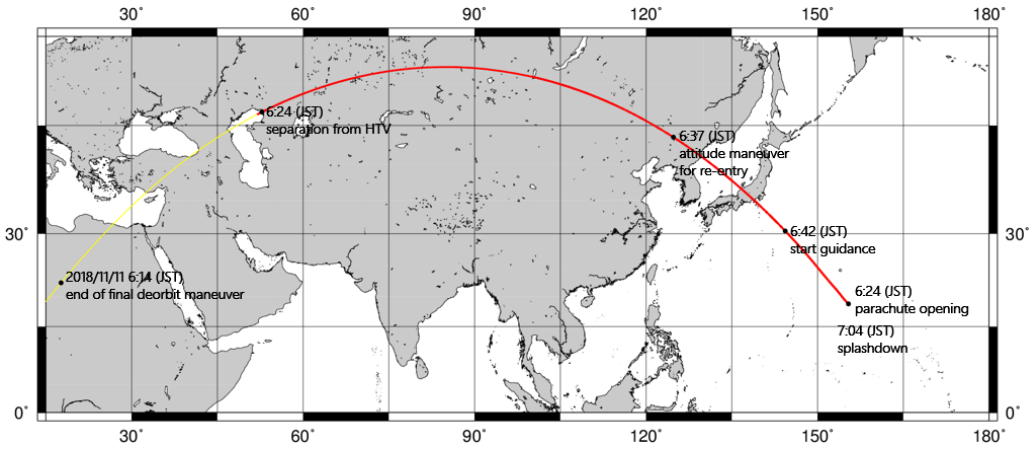

Figure 6: HSRC Mission trajectory

6.2 Evaluation of aerodynamic acceleration during flight

The mission requirement of maximum aerodynamics acceleration during flight is less than 4.0G. Figure 7 shows the magnitude of aerodynamics acceleration profile (pre-analysis simulation and flight data). The magnitude was given as $(x^2+y^2+z^3)/9.81$, where x, y, and z are the detected acceleration values of each axis, respectively. The flight results were in good agreement with the pre-analysis simulation results. The maximum aerodynamics acceleration during actual flight was 3.5G. Thus, HSRC achieved its mission. The spike in acceleration was the acceleration at separation from HTV7.

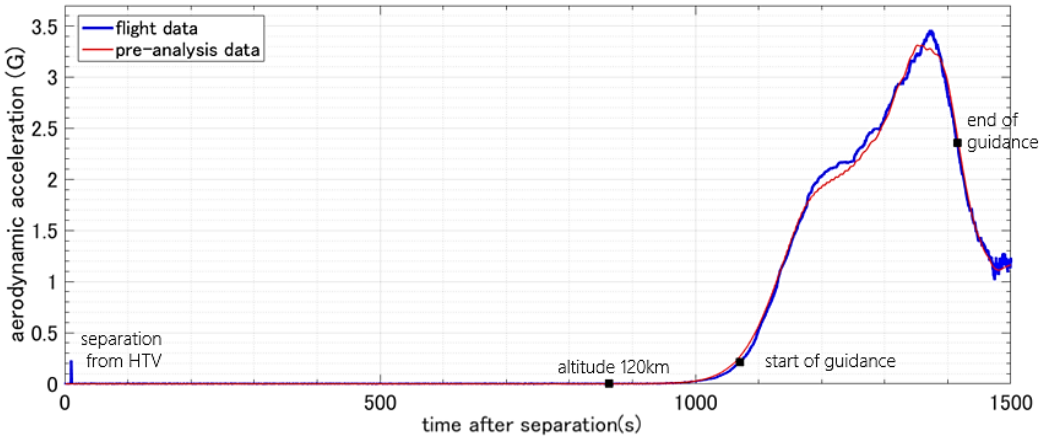

Figure 7: Magnitude of aerodynamics acceleration profile

6.2 Performance of guidance and control

We evaluated the guidance accuracy excluding navigation error at guidance termination, because updating the navigation value by GPS failed. Figure 8 shows the navigation trajectory and the target-point. The error from target-point at termination guidance is divided into three errors. Figure 8 shows the down-range error, the cross-range and the altitude error in local horizontal coordinate system. The altitude error was 0.19km. The down-range error was 0.51km. The cross-range error was 8.29km. From the flight results, we evaluated that the guidance accuracy of down-range was sufficiently high. Conversely, the cross-range error was within 10km but large. This is because the cross-range error is determined by the final bank reverse timing in the guidance logic. Further studies on the guidance logic are thus needed to achieve more guidance accuracy.

DOI: 10.13009/EUCASS2019-428

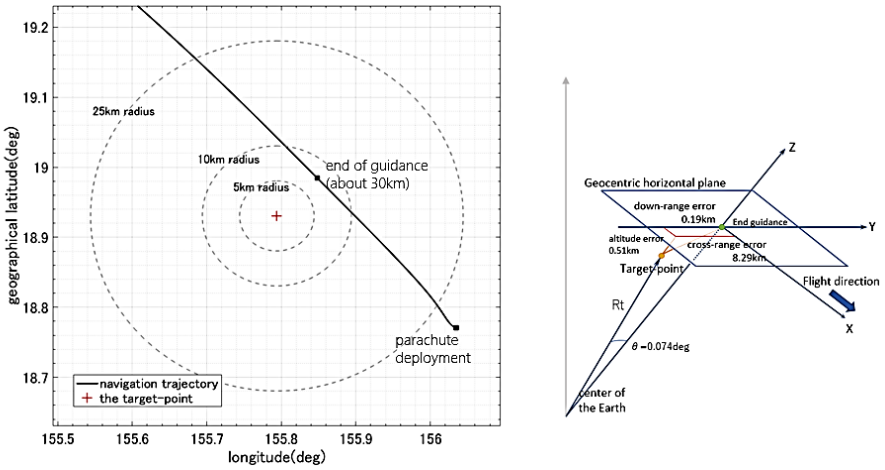

Figure 8: Relationship between the navigation trajectory and the target-point

6.3 Bank angle modulation by range prediction in real-time using numerical integration

Figure 9 shows the bank commands and navigation values. The GN&C system including the guidance logic performed bank angle modulation to reduce the down-range error. The HSRC flight performed four bank reversals (see Fig. 10). The actual flight was avoided as designed to avoid bank reversal in two ground speed ranges: Mach 1 and ground speed of 2000-3000m/s. Moreover, a comparison of the actual flight data and the pre-analysis revealed the following:

(1) The initial attitude navigation error
As HSRC was not equipped with any absolute attitude sensor (e.g., STT), its attitude could not be calibrated before re-entry. Therefore, the pre-analysis found that the initial attitude error adversely affects guidance accuracy. from the flight data, it was assumed that attitude angle error did not exceed design range 3σ.

However, we consider that the attitude angle 'roll+' error was large. This is because overshoot of the bank angle command can be confirmed after bank reversal to a plus bank angle. Conversely, an overshoot after bank reversal to a minus bank angle cannot be confirmed. Based on our analysis, such overshoot occurs in case of roll+ initial angle error. The roll initial angle error leads to L/D navigation error that depends on the sign of the bank angle. The L/D navigation values are used for guidance calculations (see the section 5.2). As a result, the predict-range error is large before and after bank angle reversal, and overshoot occurs immediately after bank angle reversal.

(2) Rolling moment coefficient
There is a bias of approximately 3 degrees between the navigation value and the command (see Fig. 9). And the control kept blowing the roll thrusters against the disturbance torque. Based on our analysis, the rolling moment coefficient causes a steady disturbance torque in the roll direction. Therefore, a rolling moment (+) is considered to have occurred in actual flight. The flight result suggests the need to consider rolling moment coefficient in the design of GNC system.

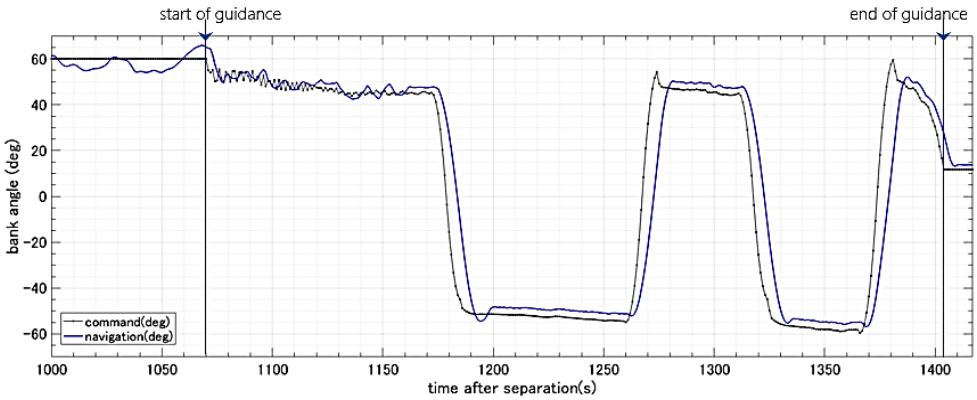

Figure 9: Bank angle profile (black line: command, blue line: navigation data)

DOI: 10.13009/EUCASS2019-428

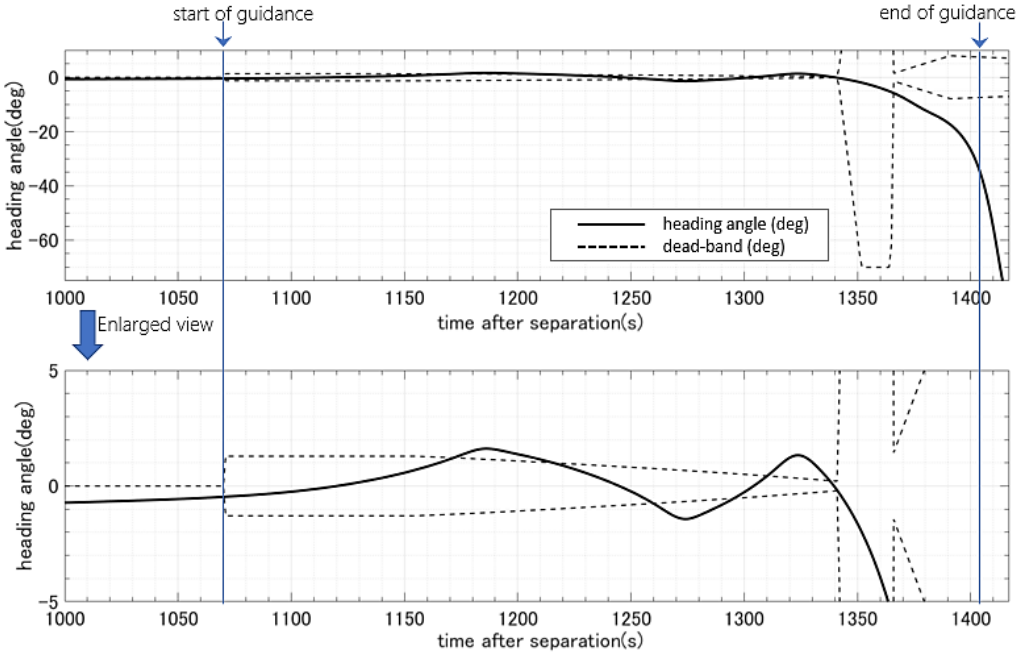

Figure 10: Heading angle profile

6.4 longitudinal motion in the transition flow

In this section, we discuss the longitudinal motion, particularly the attack angle behavior in the transition flow. Figure 11 shows the attack angle profile. The command was designed to output the trim angle scheduled by ground speed. In the longitudinal motion during the transitional flow, the “head-up” that was not expected at the time of design occurred as shown in Fig. S. The following points regard to “the Head-up” are understood from the flight data.

- The head-up changes at a rate of about 0.9 deg/s.
- The common logarithm of Knudsen number ($\log_{10}$Ku) is about -1.0 to 0.0 when the head-up occurred.
- As the HSRC was not controlled by using the thrusters while raising the head, a disturbance moment was thus considered to be applied to the HSRC.

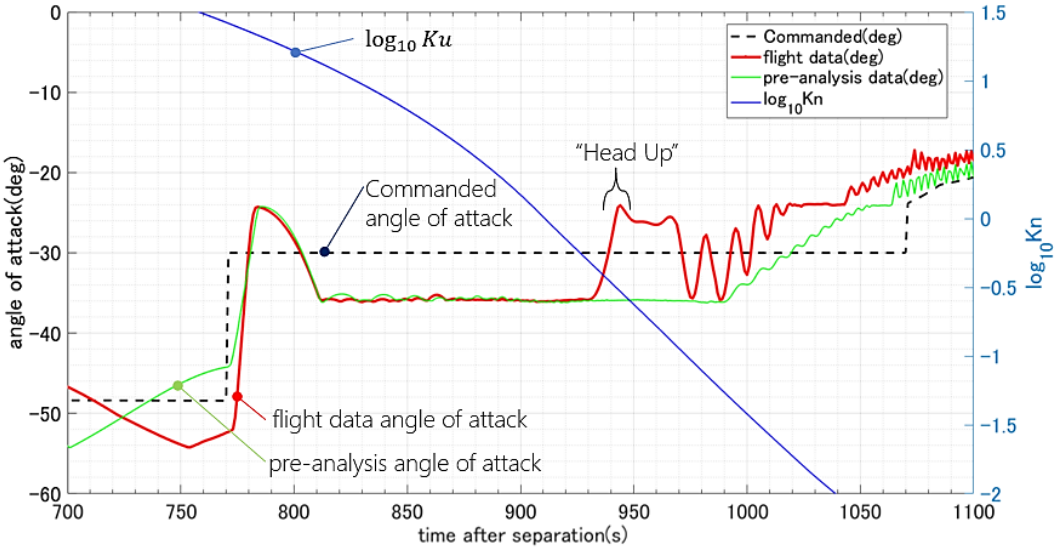

Figure 11: The attack angle profile in the transition flow

DOI: 10.13009/EUCASS2019-428

We assumed that multiple factors caused the disturbance moment. The first factor is the effect of Multi Layer Insulation (MLI) burn-off. This effect refers to the possibility that there was a burnt-off of MLI at the lower part of the body, which became a protrusion and caused the disturbance moment. The second factor is aerodynamic model error, where the trim angle in the transitional flow is different from the design. The third factor is the influence of gas generated from the ablator. The head-up occurred when aerodynamic heating started to increase. And a disturbance moment may have possibly occurred due to ablation changing the flow around the capsule. The evaluation of the HSRC in terms of aerodynamic design is given in [13].

As the cause of this head-up has not been explained, we need further research to clarify the cause of this HSRC behavior in the transitional flow. The challenge of achieving a more stable and secure re-entry of the small capsule entails improving the accuracy of the simulation model during the transitional flow.

6.5 Evaluation of fuel consumption

Figure 12 shows the results of comparing the flight data and the pre-analysis profile on fuel consumption. The pre-analysis profile is the nominal profile with all no error. The fuel consumption of the actual flight increased compared to that of the nominal as shown in Fig. 12 Fuel consumption is increased compared to the nominal trajectory as shown in Fig. 12. We consider the factors that increased fuel consumption to be as follows:

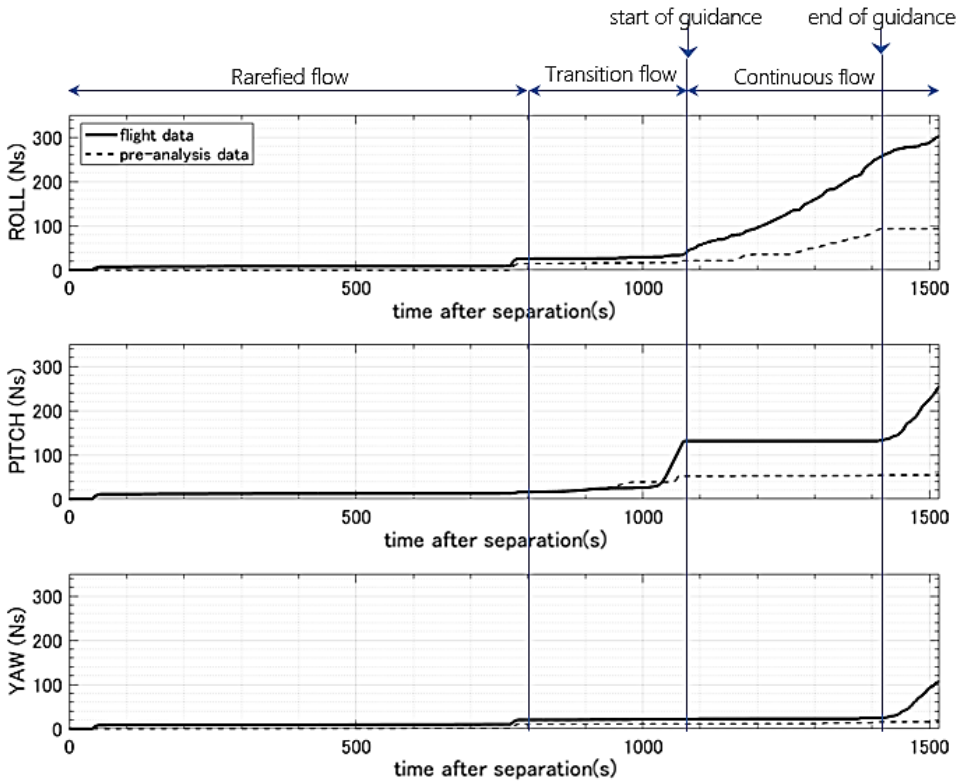

Figure 12: Fuel consumption profile (Total impulse (Ns))

- The fuel consumption for roll and yaw increased immediately after separation. HSRC was tumbling after separation and then controlled to return its attitude angle to LVLH attitude. As the result, the injection amount in roll and yaw increased.
- During the continuous flow, fuel consumption for the roll increased as shown in Fig. 12. We consider the cause of this increase to be the continued blowing of the roll thrusters against the disturbance torque due to the rolling moment coefficient (see 6.3).
- During flight from the transition flow to the continuous flow, the fuel consumption of pitch increased. We consider that the transition, from the transitional flow to the continuous flow was faster than expected at design. Specifically, there was a difference between the command trim angle and the navigation value (i.e., actual trim angle). As a result, the pitch thruster kept blowing to follow the commanded attitude (see Fig. 11), thereby increasing the fuel consumption for pitch.

DOI: 10.13009/EUCASS2019-428

7. Trajectory reconstruction

Purpose and approach

"Trajectory Reconstruction" in this paper refers to reproducing the actual flight behavior with the 6-degree-of-freedom flight simulator which was used in the verification of HSRC GN&C. The trajectory reconstruction has two purposes. The first is to estimate the actual trajectory for evaluating the aerodynamic database. The second is to evaluate the validity of the flight simulation model assumed in design. The validity of the design verification method of HSRC is confirmed by comparing the actual flight results and the reconstructed trajectory. The evaluation results are then used as feedback for a future design method.

In order to reproduce an actual flight with the flight simulator, the simulation models should represent the actual flight environment precisely. Here, the models are, for example, a density model, an aerodynamic database of capsules, and a sensor model. In the scope of this paper, we assumed that the difference between actual flight environment and the simulator model can be represented only by bias error of each model. Then, by estimating the error value, we try to reproduce the actual flight behavior by the simulator.

The error parameters to be estimated are selected by comparing the flight simulation (single error analysis) with the flight data. The following sources of error are assumed to have occurred during actual flight.

(1) Initial attitude navigation error
(2) Gyro bias error
(3) Error of density
(4) Axial force coefficient error
(5) Normal force coefficient error
(6) Pitching moment coefficient error
(7) Rolling moment coefficient error

These errors are estimated so that output of the simulator matches the actual flight result.

Trajectory reconstruction

We first estimate the initial attitude navigation error and gyro bias error. As HSRC unfortunately failed in initial acquisition of GPSR, the only navigation-related data obtained in this demonstration is the IMU data.
However, the exact time and position of splashdown are known. Therefore, these errors are estimated so that the landing position and landing time obtained by inertial navigation calculation using the IMU data (gyro, acceleration) will match the actual flight results.

The left figure shows the trajectory before estimation, and the right figure shows it after estimation. The trajectory after estimation indicates that the landing position is well matched. The roll error estimation result is +0.6 deg. The error is estimated as a positive error and is consistent with the discussion in Section 6.4.

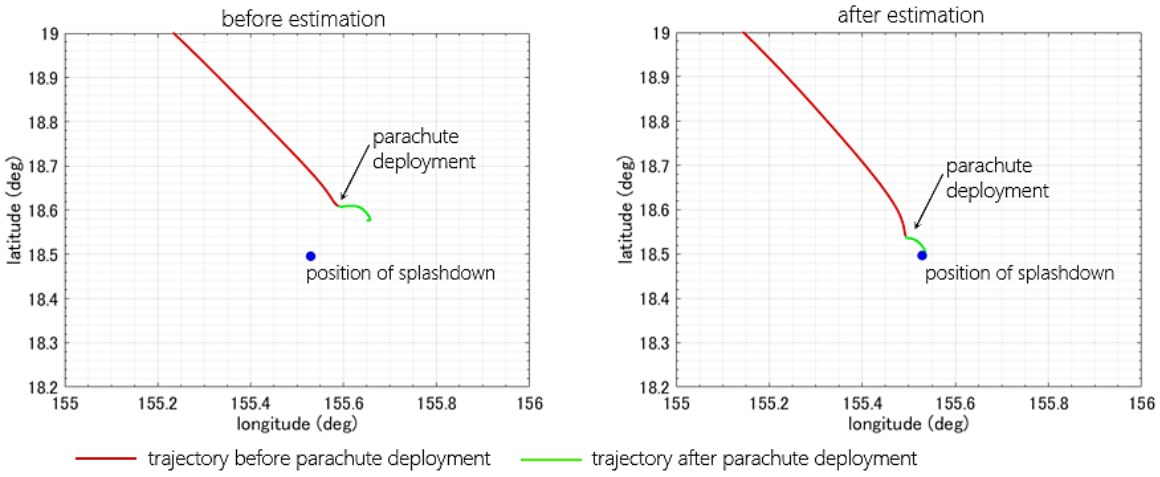

Figure 13: Trajectory reconstruction by correction the initial attitude navigation error and gyro bias error

DOI: 10.13009/EUCASS2019-428

Next, the density error and aerodynamic error are estimated by combinational optimization. The combined optimization method used the downhill simplex method. The initial attitude navigation error and gyro bias error are not included in the estimation parameters of combinatorial optimization, but use the results obtained as described in the previous paragraph. The evaluation function considered the navigation value and the bank angle command. The errors were estimated so that the navigation values and bank angle commands obtained from the simulation results match the actual flight data. The rolling moment coefficient error estimation result is + 0.6σ. The error is estimated as a positive error and is consistent with the discussion in Section 6.5

Figure 14 shows the trajectory reconstruction obtained using the estimation errors. The actual flight can be roughly simulated for the bank angle command and navigation value as shown in the figure. However, the start timing guidance and the value of the bank angle command in the final re-entry phase are still low in reproduction accuracy. In order to reproduce an actual flight with higher accuracy, the simulator model must be correlated.

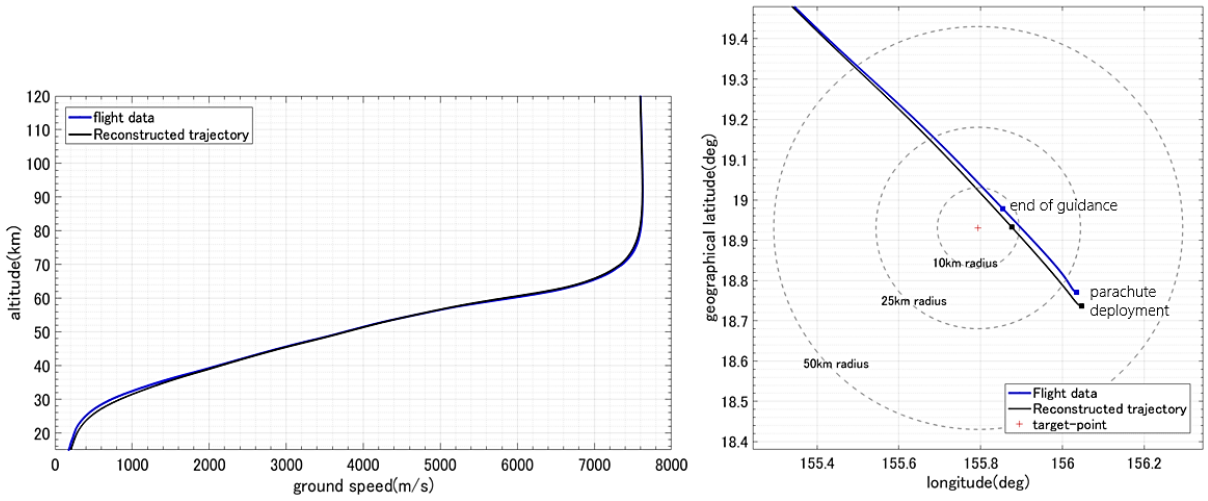

Figure 14(a): Navigation value comparison of flight data and orbital reconstruction
(the left figure : ground speed-altitude navigation profile, the right figure : navigation trajectory)

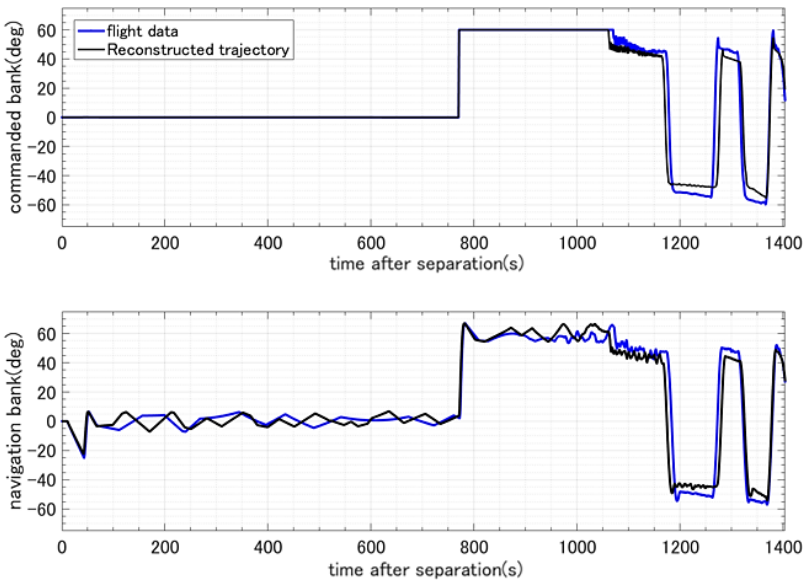

Figure 14(b): Bank angle comparison of flight data and orbital reconstruction
(the upper figure : bank comand prifile, the lower figure : bank angle navigation profile)

DOI: 10.13009/EUCASS2019-428

8. Conclusion and future work

HSRC was successful in recovering the capsule including the samples from ISS in November 2018. In this paper, we presented the design of the GN&C system of HSRC and describe the post-flight evaluation results of the guidance and control. One of the key designs of GN&C system is the re-entry guidance logic. The logic is based on range prediction in real-time using numerical integration, and calculates flight range sensitivity to correct bank angle. The flight results suggested that the proposal guidance logic is effective for reducing of maximum aerodynamic acceleration during re-entry flight and improving of guidance accuracy.

Although the flight results were sufficiently successful, we consider that there are three issues remain. The first is a demonstration of IMU/GPSR-nav, which can be expected to improve the guidance accuracy. The second is to modify the guidance logic for improving the cross-range accuracy. The third issue is the correlation of the aerodynamic model in the transitional flow. Further work needs to achieve higher accuracy and certainty in the future.

Acknowledgements

I would like to convey my sincere thanks to Mr. Hirokazu Suzuki for giving valuable advice in designing the GN&C system of HSRC.

References

[1] http://iss.jaxa.jp/en/htv/mission/htv-7/181205_interview.html
[2] Matsumoto, S., Suzuki, H., Izumi, T., Mori, T., Sugano, K., Wakamiya, M., and Mitsui, S. Evaluation of the Guidance, Navigation and Control System for OREX. Special Report of National Aerospace Laboratory, SP-24, pp.117-130, 1994.
[3] Matsuda, S., Makino, T., Ijichi, K., and Shingu, S. Results of Reentry Flight Trajectory of USERS. Proc. of 13th workshop on Astrodynamics and Flight mechanics, 2003.
[4] Kazuhiko Yamada, Tetsuya Yamada, Masatoshi Matsuoka. EDL analysis for "HAYABUSA" reentry and recovery operation. Proc. Of 20th workshop on Astrodynamics and Flight Mechanics, 2010
[5] Bogner, I., Description of Apollo Entry Guidance, NASA TM-66-2012-2, August 1966.
[6] Graves CA, Harpold JC. Apollo experience report—mission planning for Apollo entry. Technical Report, NASA Technical Note, TND-6725; March 1972.
[7] Barth, Andrew, Mamich, Harvey, Hoelscher, Brian, "POST-FLIGHT ANALYSIS OF THE GUIDANCE, NAVIGATION AND CONTROL PERFORMANCE DURING ORION EXPLORATION FLIGHT TEST 1" Advances in the Astronautical Sciences, Guidance, Navigation, and Control 2015, Vol 154, pp. 931-943
[8] PutnamZR, NeaveM, BartonG. Predguid entry guidance for orion return from low earth orbit. In: IEEE aerospace conference, IEEEAC1571, BigSky, MT; 2010.
[9] G.F. Mendeck, L.E. Craig, Entry guidance for the 2011 Mars Science Laboratory Mission, in AIAA Atmospheric Flight Mechanics Conference and Exhibit, Portland, Oregon Aug. 8–11 2011. AIAA 2011-6639
[10] G. Mendeck and L. McGrew, "Post-Flight EDL Entry Guidance Performance of the 2011 Mars Science Laboratory Mission," AAS 13-419, AAS/AIAA 23rd Space Flight Mechanics Meeting, Kauai, HI, Feb. 2013.
[11] Shuichi Matsumoto, Yoshinori Kondoh, Yusuke Suzuki, Hifumi Yamamoto, Satoshi Kobayashi, and Noboru Motoyama. Accurate Real-Time Prediction Guidance Using Numerical Integration for Reentry Spacecraft. Proc of AIAA Guidance, Navigation, and Control Conference, AIAA-2013-4646,2013
[12] Bibb, K. L., Walker, E. L., Brauckmann, G. J., and Robinson, P. E. 2011. Development of the Orion Crew Module Static Aerodynamic Database, Part II: Supersonic/Subsonic. 29th AIAA Applied Aerodynamics Conference, Honolulu, HI, 27-30 June 2011, American Institute of Aeronautics and Astronautics, Reston, VA (submitted for publication).
[13] Keiichiro, F., Takayuki, I., Hideyo, N., Ryoh, N., Kawashima, I., Yasuhide, W., Kota T., Computational Aerothermodynamics for HTV Small Re-entry Capsule Project, 8th EUCASS, 2019.